

MeV mass sterile neutrino decay at short-baseline neutrino facilities

One Two Three

Institute for Particle Physics Phenomenology, Department of Physics, Durham University, South Road, Durham DH1 3LE, United Kingdom

E-mail: one@durham.ac.uk, two@durham.ac.uk, three@durham.ac.uk

ABSTRACT: We study the sensitivity of the Short-Baseline Neutrino (SBN) programme at Fermilab to sterile neutrino decay in a variety of models. We show that this experimental complex can be expected to extend the known bounds on such decays and comment on the interplay between the different beam lines and detector technologies.

Contents

1	Introduction	1
2	Short-Baseline Neutrino Complex	1
3	Sterile neutrino decay	2
4	Simulation details	4
4.1	Sterile neutrino fluxes	5
4.2	Detector modelling and analysis cuts	6
4.3	Background modelling	7
4.3.1	πe and $\pi\mu$ channels	7
4.3.2	e^+e^- single and double track channels	9
4.3.3	$\pi^0\nu_\alpha$	10
5	Sensitivities	11
6	Conclusions	11
7	To do list	12

1 Introduction

Lorem ipsum dolor sit amet, consectetur adipiscing elit, sed do eiusmod tempor incididunt ut labore et dolore magna aliqua. Ut enim ad minim veniam, quis nostrud exercitation ullamco laboris nisi ut aliquip ex ea commodo consequat. Duis aute irure dolor in reprehenderit in voluptate velit esse cillum dolore eu fugiat nulla pariatur. Excepteur sint occaecat cupidatat non proident, sunt in culpa qui officia deserunt mollit anim id est laborum. Lorem ipsum dolor sit amet, consectetur adipiscing elit, sed do eiusmod tempor incididunt ut labore et dolore magna aliqua. Ut enim ad minim veniam, quis nostrud exercitation ullamco laboris nisi ut aliquip ex ea commodo consequat. Duis aute irure dolor in reprehenderit in voluptate velit esse cillum dolore eu fugiat nulla pariatur. Excepteur sint occaecat cupidatat non proident, sunt in culpa qui officia deserunt mollit anim id est laborum.

2 Short-Baseline Neutrino Complex

¹ The Fermilab SBN programme [1] will comprise of a number of detectors in the Booster Neutrino Beam (BNB): SBND (previously known as LAr1-ND) at 100m from the target, MicroBooNE at 470m and ICARUS-T600 at 600m.

¹PB: This could also be bundled into the intro...

In addition to events arising from the BNB, the detectors of the SBN complex will also collect events associated with the NuMI beam, currently being used in the NO ν A, MINER ν A and MINOS+ experiments.

3 Sterile neutrino decay

Generically, a gauge-singlet fermion will be unobservable by all non-gravitational means unless it mixes with the active neutrino sector. The presence of mixing introduces a range of possible observable signatures depending on the magnitude of the sterile mass and its mixing to the active sector.

The most general renormalizable lagrangian extending the SM to include a single novel gauge-singlet fermion N is given by

$$\mathcal{L} = \mathcal{L}_{\text{SM}} + \bar{N} i \not{\partial} N + \frac{\mu}{2} \bar{N}^c N + \left(y_\alpha \bar{L}_\alpha \tilde{H} N + \text{h.c.} \right), \quad (3.1)$$

where y_α denote Yukawa couplings and μ a Majorana mass term for N . The extension to multiple new fermions involves promoting y and μ to matrices with indices for the new states, but will offer no real phenomenological differences in the current work.¹ Much work has been done understanding the phenomenology of novel neutral states, which varies significantly over their large parameter spaces. An important signal for light sterile neutrinos are possible observable effects in oscillation experiments, which could alleviate short-baseline oscillation anomalies; although, no minimal solution seems to provide a particularly compelling improvement []. At larger masses, the neutral particles no longer participate in oscillation, but these models can generate new signatures at beam dump experiments []. At even higher masses, these particles could provide a natural way to suppress the size of active neutrino masses through the Type I or III see-saw mechanisms [].

Generally speaking, once the neutrinos are massive enough to no longer oscillate but remain light enough to be produced in terrestrial experiments, the best way to observe them is through their direct decay into SM particles. In the minimal lagrangian in Eq. (3.1), the only direct couplings to new sterile fermions are neutrino Higgs interactions. However, these couplings generate off-diagonal neutrino bilinears below the electroweak symmetry breaking scale, which leads to mixing between the 4+ flavours of neutrinos. Such mixing then introduces production and decay mechanisms of many kinds for the state N through mass insertion on an active neutrino fermion line. These decays have been studied extensively in the literature [?] and depend only on the size of neutrino mixing to various flavours, parameterized by the elements of an extended 4×4 PMNS matrix,

$$U_{e4}, \quad U_{\mu 4} \quad \text{and} \quad U_{\tau 4},$$

and the mass of the state N itself. The branching ratios for these decays are shown in Fig. 1 as a function of mass for two extremes of the flavour mixing pattern. On the left, we show

¹The minimal single N extension does not allow for the observed masses of the neutrinos, as the mass matrix is rank 1. We assume that an appropriate extension has been performed to satisfy neutrino oscillation data.

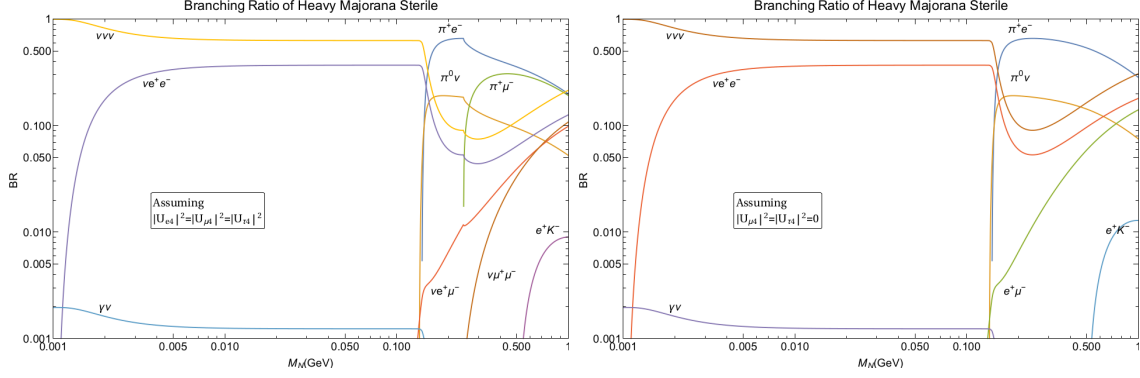


Figure 1. The branching ratios for sterile neutrino decays in the minimal 3 sterile SM extension. The left panel assumes equal mixing with all active flavours, whilst the right panel assumes a flavour hierarchical scheme where only the mixing with ν_e is important.

the branching ratios if the new state only mixes with all flavours of active neutrino equally $U_{e4} = U_{\mu 4} = U_{\tau 4}$, and on the right, when the only mixing with ν_e ($U_{\mu 4} = U_{\tau 4} = 0$). The main effect of the flavour structure is to forbid certain decays which require certain elements. For example, the decay of a sterile N into a lepton and a charged pion,

$$N \rightarrow l^\pm \pi^\mp,$$

only proceeds if $U_{l4} \neq 0$. This, in turn, affects the possible production mechanisms for these particles. In a conventional neutrino beam, most neutrinos are derived from meson decay (or secondary μ^\pm decays). If $U_{e4} = U_{\mu 4} = 0$, such decays with a mass insertion for the sterile neutrino are impossible for pions or kaons. For this reason, we will mainly focus on mixing with the first two generations. This parameter space will be probed by working at higher energies, where the neutral fermions can be produced by decays of charmed mesons such as D^\pm , by the SHiPS experiment [1].

We highlight four decays in our study. These have the largest branching ratios of all channels with visible decay products over the mass range $m_s \lesssim 1$ GeV. This is based on the minimal sterile extension of the SM discussed above, but we stress that similar decays can occur in any number of non-minimal models, where the relationship between decay rate, mass and mixing can be non-standard. For sterile neutrino masses less than the pion mass, the dominant visible decay will be into an electron-positron pair as can be seen from Fig. 1. The decay rate for this channel is given by

$$\Gamma(\nu_s \rightarrow \nu_i e^+ e^-) = \frac{G_F^2 m_s^5}{96\pi^3} I(m_s, U^2).$$

where $I(m_s)$ is an integral. [We'll have to decide how to type these things in.](#) We will base two analyses on this channel, differentiated by the number of tracks we expect to see. The first event sample will attempt to measure events where two tracks are resolved, which is expected to have a small background but favours low-energy events. The second sample studies the converse, where only a single track can be seen, predominately due to a tightly collimated e^+e^- -pair. In this case we expect a larger background (from anything producing

a single track), but as we will show, we get sizable event numbers in this channel due to the sterile neutrino’s high energy, and a tight cut on the angular distribution can make it sensitive to sterile decays.

When the mass of the sterile neutrino is greater than the kinematic threshold for the production of a neutral pion, a new decay dominates $\nu_s \rightarrow \nu_i \pi^0$. The decay rate for this process is given by

$$\Gamma(\nu_s \rightarrow \nu_i \pi^0) = \frac{G_F^2 f_\pi^2 m_s^3}{64\pi} \left[1 - \left(\frac{m_\pi}{m_s} \right)^2 \right].$$

The next channel appears at the kinematic threshold for charged pion production with a charged lepton. If mixing between the heavy mass state and the electron neutrino is present, this decay occurs almost immediately after the $\nu\pi^0$ channel opens. However, if this mixing is negligible, there is a the size of the muon mass before the $\mu^\pm \pi^\mp$ channel opens. As can be seen from Fig. 1, these decays dominate the visible decays when they are allowed. These decays have a similar scaling behaviour of the decay rate to the $\nu\pi^0$ channel with an equivalent dependence on the pion structure constant,

$$\Gamma(\nu_s \rightarrow l^\pm \pi^\mp) = |U_{l4}|^2 \frac{2G_F^2 f_\pi^2 m_s^3}{16\pi} I(m_s).$$

Lorem ipsum dolor sit amet, consectetur adipiscing elit, sed do eiusmod tempor incididunt ut labore et dolore magna aliqua. Ut enim ad minim veniam, quis nostrud exercitation ullamco laboris nisi ut aliquip ex ea commodo consequat. Duis aute irure dolor in reprehenderit in voluptate velit esse cillum dolore eu fugiat nulla pariatur. Excepteur sint occaecat cupidatat non proident, sunt in culpa qui officia deserunt mollit anim id est laborum. Lorem ipsum dolor sit amet, consectetur adipiscing elit, sed do eiusmod tempor incididunt ut labore et dolore magna aliqua. Ut enim ad minim veniam, quis nostrud exercitation ullamco laboris nisi ut aliquip ex ea commodo consequat. Duis aute irure dolor in reprehenderit in voluptate velit esse cillum dolore eu fugiat nulla pariatur. Excepteur sint occaecat cupidatat non proident, sunt in culpa qui officia deserunt mollit anim id est laborum.

4 Simulation details

We have computed the fluxes and simulated event numbers for each beam and detector via a custom Monte Carlo program. The program allows efficiencies to be taken into account due to experimental details of the detector and its capabilities in a fully correlated way between observables.

The fluxes from BNB are taken from REF, and we assume no spectral modifications associated with the altered kinematics of the new sterile neutrino final state. Given the spectral flux of sterile neutrinos in the BNB, $d\phi/dE$, we compute the total number of accepted events in channel “c” via the following summation,

$$N_c = \sum_i \left. \frac{d\phi}{dE} \right|_{E_i} P_D(E_i) W_c(E_i),$$

where $P_D(E)$ is the probability for a sterile of that energy to reach and then decay inside the detector labelled D. The simplest approximation is to ignore all geometric effects, so that every particle travels exactly along the direction of the beam line, which gives the following probability

$$P_D(E) = e^{-\frac{\Gamma_T L}{\gamma\beta}} \left(1 - e^{-\frac{\Gamma_T \lambda}{\gamma\beta}}\right) \frac{\Gamma_c}{\Gamma_T},$$

where Γ_T (Γ_c) denotes the rest-frame total decay width (decay width into channel c), m the mass of the sterile neutrino, and L (λ) the distance to (width of) the detector. The combination $\gamma\beta$ is the usual special relativistic function of velocities of the parent particle and provides the sole energy dependence of the expression

$$\frac{1}{\gamma\beta} \equiv \frac{m}{\sqrt{E^2 - m^2}}.$$

As we are exploring a large parameter space, often this expression takes a simplified form depending on the size of $\Gamma_T \lambda / \gamma\beta$:

$$\begin{aligned} \Gamma_T \lambda \ll 1 & \quad P_D \approx e^{-\frac{\Gamma_T L}{\gamma\beta}} \frac{\Gamma_c \lambda}{\gamma\beta} + \mathcal{O}(\Gamma_T^2 \lambda^2), \\ \Gamma_T \lambda \gg 1 & \quad P_D \approx e^{-\frac{\Gamma_T L}{\gamma\beta}} \frac{\Gamma_c}{\Gamma_T} + \mathcal{O}\left(\frac{1}{\Gamma_T \lambda}\right), \end{aligned}$$

where the rate for slowly decaying particles can be seen to grow with detector size until a width of $\lambda \sim \Gamma_c^{-1}$ where longer detectors make no difference, as most steriles decay within a few decay lengths and therefore we see a fixed fraction of the total events in our channel of interest. We will comment on how the three detectors of the SBN complex can use the dependence on E and L in these expressions to enhance their sensitivity in Section ??.

Finally, the function $W_c(E)$ is a weighting factor which accounts for all effects which reduce the number of events in the sample: for example, analysis cuts or detector performance effects. To compute these factors, we run a Monte Carlo simulation of the decays for a large number of sample events with a given energy. Each sterile event is associated with a decay of type c. We then apply experimental analysis cuts to the decays based on our assumptions about the detector's capabilities and backgrounds, to produce a spectrum representing the final event sample. The percentage of accepted events defines the weight factor for that energy.

We also work spectrally producing the expected distributions of observed events. This can be used to suggest improved analysis cuts based on the interplay between the three detectors of the SBN complex. We return to this in section II.

4.1 Sterile neutrino fluxes

To leading order in the mass of the sterile neutrino over the pion, the fluxes for the ν_s will be a rescaling of the fluxes for the active neutrinos. We take these fluxes as our input and scale them by $U_{\mu 4}$, with an additional kinematic factor to take into account the helicity un-suppression of $\pi^+ \rightarrow e^+ \nu_s$ for massive $\nu_s \gg m_e$, such that for a sterile produced from the decay of a meson M

$$\phi_{\nu_s} \approx \phi_{\nu_\alpha} |U_{\alpha 4}|^2 \frac{\Gamma(M \rightarrow \nu_s \alpha)}{\Gamma(M \rightarrow \nu_\alpha \alpha)}.$$

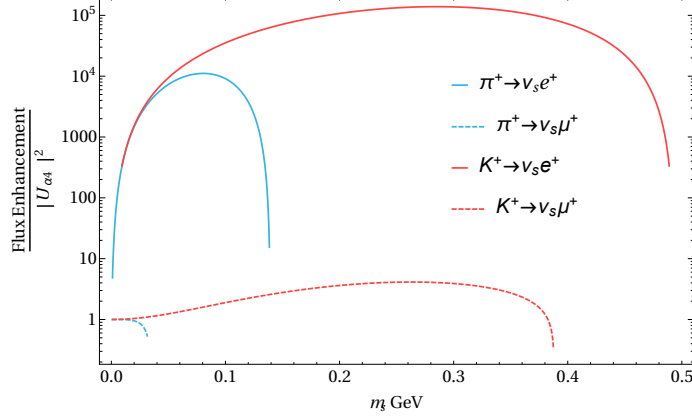


Figure 2. Kinematic enhancements of the sterile flux, for the four production channels available for steriles in the BNB beam. There is little effect when mixing with muons alone, as the muon is heavy enough to remove the helicity suppression that usually kills the $\pi \rightarrow e\nu$ channels. This factor of up to 10^5 enhancement more than compensates for the smaller flux of ν_e inherent in the BNB beam.

This kinematic effect for the pion and kaon, the only mesons produced in large numbers in the BNB beam, is shown below in figure 2

Can we add a figure of the fluxes? Perhaps some comment on how we are modelling them. This is all finished, right? (Unless we start doing something wild with the NuMI fluxes). Lorem ipsum dolor sit amet, consectetur adipiscing elit, sed do eiusmod tempor incididunt ut labore et dolore magna aliqua. Ut enim ad minim veniam, quis nostrud exercitation ullamco laboris nisi ut aliquip ex ea commodo consequat. Duis aute irure dolor in reprehenderit in voluptate velit esse cillum dolore eu fugiat nulla pariatur. Excepteur sint occaecat cupidatat non proident, sunt in culpa qui officia deserunt mollit anim id est laborum. Lorem ipsum dolor sit amet, consectetur adipiscing elit, sed do eiusmod tempor incididunt ut labore et dolore magna aliqua. Ut enim ad minim veniam, quis nostrud exercitation ullamco laboris nisi ut aliquip ex ea commodo consequat. Duis aute irure dolor in reprehenderit in voluptate velit esse cillum dolore eu fugiat nulla pariatur. Excepteur sint occaecat cupidatat non proident, sunt in culpa qui officia deserunt mollit anim id est laborum.

4.2 Detector modelling and analysis cuts

To compute the weighting factors W_c , we generate a large number of Monte Carlo events of the decay that we are interested in and remove those events which fail a series of cuts. These cuts are designed to reflect both genuine analysis cuts designed to enhance the signal to background ratio (for example, choosing events with energies within certain ranges), as well as cuts which provide a basic model of detector effects and limitations (for example, discarding events that wouldn't be reconstructed correctly, *e.g.* those with overlapping tracks in a two particle final state).

We summarize our cuts in Table 1.

Signal	Constraint	Value
e^+e^- (two tracks)	low-energy thresh.	50 MeV
	foreshortened angular separation	$> 5^\circ$
	energy ratio $E_{\text{low}}/E_{\text{high}}$	> 0.1
	angle?	100%
e^+e^- (single track)	low-energy thresh.	50 MeV
	foreshortened angular separation	$< 5^\circ$
	energy ratio $E_{\text{low}}/E_{\text{high}}$	< 0.1
	angle?	100%
$\pi^+e^-(\pi^-e^+)$	low-energy thresh.	10 MeV
	energy ratio E_e/E_π	> 0.1
	angle?	100%
$\pi^+\mu^-(\pi^-\mu^+)$	low-energy thresh.	10 MeV
	energy ratio E_μ/E_π	> 0.1
	angle?	100%

Table 1. Detector cuts as modelled in our simulation.

4.3 Background modelling

For each channel, we have implemented a model of the dominant backgrounds. The properties of these backgrounds will motivate our cuts. The knowledge of the background and the cuts to motivate a reasonable estimate of the backgrounds to the searches of interest. We will discuss the details of the modelling that we have performed in a channel-by-channel basis. The results of this rate only background analysis is summarised in Table (2) below.

4.3.1 πe and $\pi\mu$ channels

Pions produced inside MicroBooNE will quickly decay into muons, which subsequently decay into Michel electrons. We can expect this chain of decays to be well reconstructed in liquid argon, and the dominant backgrounds to the sterile decays we are interested in will be genuine π -lepton production associated with the neutrino beam. So-called CC1 π^+ events are defined as the associated production of a charged pion from the standard CC process which produces a lepton. This can happen by resonant production, where a nucleon is excited into an unstable state, for example into a Δ , and the following decay produces a nucleon and a pion. Such decays are characterised by a isotropic spectrum due to the relatively mild boost of the resonant state [?]. Another contribution to the cross-section is from coherent scattering, where the neutrino scatters from the whole nucleus

$$\nu_l + A \rightarrow l^- + A + \pi^+ \quad \text{or} \quad \bar{\nu}_l + A \rightarrow l^+ + A + \pi^-.$$

These interactions tend to produce more forward decay products and will be the dominant source of our backgrounds. Cross-sections for these processes have been studied in Mini-BooNE [?] and MINER ν A [?] and cross-sections appear to agree with Monte Carlo calculations based on the Rein-Sehgal model [? ?].

Signal	Cut	BG Event Rate
e^+e^- (two tracks)	No Cuts	3082
	$E > 200$ MeV	1055
	No Vertex	152
e^+e^- (single track)	No Cuts	1926
	No Hadronic Activity	1492
	$E > 100$ MeV	186
	<u>1γ BKG</u>	+954?
$\pi^+\mu^-(\pi^-\mu^+)$	No Cuts	≈ 40000
	No Hadronic Activity	5055
	m_μ forward supression	4034
	Estimated Angular Cut	2000
$\pi^+e^-(\pi^-e^+)$	No Cuts	310
	No Hadronic Activity	106
$\pi^0\nu_\alpha$	No Cuts	9093
	No Hadronic Activity	<u>1697 Coherent only</u>

Table 2. Estimated background rates for the four channels considered in this analysis.

For each signal channel we consider the backgrounds which have the largest contribution. Here we focus on beam driven backgrounds, with the assumption that cosmogenic backgrounds are significantly less of an issue via timing and directional cuts. In all cases, requiring no nuclear effects should greatly reduce beam related charge current events, perhaps this is directly estimatable in GENIE?

Can we reduce the incoherent BG by requiring no hadronic activity? What are we sensitive to? (There is usually a flying nucleon for incoherent. Unlike coherent scattering.)

It turns out [?] that forward going events are suppressed by muon mass. Does this mean that an angular cut could kill a lot of our BG for $\pi\mu$? (Leaving only electron neutrino processes?)

Additional backgrounds to the $\pi\mu$ (πe) channels will be from the dominant backgrounds to the πe ($\pi\mu$) channel with further particle misidentification.

- $\pi^+\mu^-(\pi^-\mu^+)$

Charged coherent pion production, $\nu_\mu A \rightarrow \mu^- A\pi^+$, is large background, identical in particle content to a decaying sterile signal. Such a low Q^2 process tends to favour daughter pions and muons that are forward going, kinematically very similar to decays in flight, as well as no observable nuclear activity. ArgoNeut analysis estimates the approximate number of events, for similar liquid argon technology to μ BooNE [2] For low energy no events have been observed thus far, see SciBooNE [3] and high energy event rates are in accordance with what is expected, see NOMAD [4].

There is approximately 40,000 events coherent and incoherent resonant 1μ 1π events produced in MicroBooNE. However, when one ensure that there is no hadronic activity this reduces to 5055, 2626 of which are CC coherent events, the remainder from

incoherent events which have little or no observable hadronic activity. Any further reduction must arise from kinematic cuts. As you mentioned that forward going events are suppressed for our BG, if we include the 25% suppression for coherent and 15% for incoherent that leaves us with 4034 events. However, the real benefit here will come from out spectrum in relation the the pions. As the incoherent is relatively isotropic, the 2000 events from the coherent production will probably be our main irreducible background.

- $\pi^+e^-(\pi^-e^+)$

Coherent pion production is in theory a background similar to the muon case above, however, this process has never been experimentally measured with associated electron production, and estimated event rates in microBooNE are $\mathcal{O}(10)$ events. Thus a much larger background is any traditional $\mu\pi$ production in which the muon is mis-identified as an electron, however, this should be quite small, between 50-100 events.

4.3.2 e^+e^- single and double track channels

- e^+e^- (single tracks)

Any CCQE scattering event producing a single electron acts as a possible background to sufficiently boosted e^+e^- pairs. However, as this is a key background to the ν_e appearance oscillation analysis the kinematics and rates are well understood. The additional requirement that the single electron is not accompanied by any pions, as well as no nuclear proton recoils in which nuclear energy is above the threshold of 50 MeV (50 is probably too large, 21 is more appropriate, however, numbers exist for 50 in easier to access papers), reduces the background rate by approximately 30% to 1492 events. To further improve on this one can use the resultant electron spectral shapes. As events containing no pion or protons favour forward focused electrons, mimicking a daughter electron from a sterile decay in flight, the angular spectrum does not play a significant role in background reduction. A substantial number of these electrons-like events are not true electrons but mis-id low-energy photons from $\pi^0 \rightarrow \gamma\gamma$ decay or muons, one can apply a low energy threshold cut of 100 MeV on the electron energy to reduce the number of expected events to 186 (29 with perfect proton detection).

Hmm, two electrons overlapping have twice the $\frac{dE}{dx}$ or a single electron, so we may have to include the single photon events as described below.

- e^+e^- (two tracks)

The primary background to a resolvable e^+e^- two-track pair is either a single photon which pair produces two clean electrons rapidly such that the shower separation is not observable or a two photon system, such as from a NC $\pi^0 \rightarrow \gamma\gamma$ decay, in which both photons are mis-id as electrons. If one assumes that all single photon events can be a possible background to a e^+e^- search there is approximately 2088 events expected in 6.6×10^{20} POT. Similarly to the single track e^+e^- , most of this background is

Channel assuming 6.6×10^{20} PoT	Num Events
CCQE ($\nu_\mu n \rightarrow p\mu^-$)	60,161
NC elastic ($\nu_\mu N \rightarrow \nu_\mu N$)	19,409
CC resonant π^+ ($\nu_\mu N \rightarrow \mu^- N\pi^+$)	25,149
CC resonant π^0 ($\nu_\mu n \rightarrow \nu_\mu p\pi^0$)	6,994
NC resonant π^0 ($\nu_\mu N \rightarrow \nu_\mu N\pi^0$)	7,388
NC resonant π^\pm ($\nu_\mu N \rightarrow \nu_\mu N'\pi^\pm$)	4,796
NC coherent π^0 ($\nu_\mu A \rightarrow \nu_\mu A\pi^0$)	1,694
CC coherent π^+ ($\nu_\mu A \rightarrow \mu^- A\pi^+$)	2,626
Intrinsic ν_e CC	326
CC coherent π^+ ($\nu_e A \rightarrow e^- A\pi^+$)	9 (my estimate)

Table 3. Some estimated statistics for various channels in microBooNE, as estimated using previous MiniBooNE and ArgoNeut data.

at low energies so a 200 MeV cut on photon energy reduces this significantly to 654 events. To estimate the two photon mis-identification we apply a conservative 6% photon to electron mis-id rate to known two photon backgrounds to obtain a rate of approximately 994 events. A further cut on energy of 200 MeV on both photons reduces this to 401.

These can be naively combined to give 1055 (3082) with (without) a 200 MeV cut on photon energy. Additional backgrounds involving mis-id muons will not be significant in comparison to these NC pion decays and any remaining cosmic backgrounds not naturally removed by beam spill is eliminated by such a 200 MeV cut.

The above single photon analysis assumes the possible existence of a vertex in which to measure the photons conversion length from. In the absence of a vertex in which to measure off this can be reduced to 1389 (152) without (with) a 200 MeV energy cut.

Effect of angular cuts?

4.3.3 $\pi^0\nu_\alpha$

Although a subdominant decay mode when steriles mix with electrons alone, when one considers non-zero $|U_{\mu 4}|^2$ the branching ratio of $\nu_s \rightarrow \nu_\mu \pi^0$ becomes dominant for a mass window $\approx 140 \rightarrow 240$ MeV. Single neutral pions are produced in great numbers at the three SBN facilities, so the lack of any nuclear recoil is crucial in eliminating the majority of the incoherent neutral pion production background. The NC coherent pion production, however, does not contain any nuclear tracks and so will be an irreducible background for this channel.

5 Sensitivities

In Fig. 3 we show the sensitivity when cuts are omitted for backgroundless searches. This corresponds to the most optimistic case: there are no cuts (weight factors are set to 1, not even taking into account physical limitations on the data set) implying perfect signal efficiency, and the channels are assumed backgroundless. The analysis only considers the total number of events in each channel, and the contours mark the regions where the detectors in question see more than 2.44 events, following the procedure of Ref. [5] designed for backgroundless searches for rare events.

To investigate how the presence of backgrounds weaken these sensitivities, we have performed a rough estimate of the significance of the signal in various channels. In Fig. ??, we consider the quantity $S/\sqrt{\lambda B}$ and plot contours when the parameter is equal to 1. At this point, the size of the new signal events from the heavy sterile decays are equal to the Poisson noise in the experiment under the approximation of no signal. The parameter λ is used to scale the backgrounds, corresponding to a greater ability to suppresses these events. We show two regions, the most conservative line corresponds to $\lambda = 1$ with no additional background suppression beyond our estimates, whilst the more optimistic one corresponds to a further suppression by a factor of 1000. Our estimates are given by the largest numbers in Table 3 for each channel, that is assuming no analysis-based reduction in rates. As before, we do not take into account the signal efficiency in these plots (weight factors are set to 1) this makes the unrealistic assumption that whatever has been done to reduce the backgrounds leaves the signal event rates unchanged. However, it provides an understanding of the severity of the impact of the backgrounds for these searches.

Be careful: the contours aren't really the same thing as the shaded region, as they are computing different statistical quantities. But to make them into actual exclusion curves, we would have to minimize over the 2D space... which maybe we should do... but as we know it takes a bit of work. Also, the ee flux isn't quite right for a reason I forget at the moment.

6 Conclusions

Lorem ipsum dolor sit amet, consectetur adipiscing elit, sed do eiusmod tempor incididunt ut labore et dolore magna aliqua. Ut enim ad minim veniam, quis nostrud exercitation ullamco laboris nisi ut aliquip ex ea commodo consequat. Duis aute irure dolor in reprehenderit in voluptate velit esse cillum dolore eu fugiat nulla pariatur. Excepteur sint occaecat cupidatat non proident, sunt in culpa qui officia deserunt mollit anim id est laborum. Lorem ipsum dolor sit amet, consectetur adipiscing elit, sed do eiusmod tempor incididunt ut labore et dolore magna aliqua. Ut enim ad minim veniam, quis nostrud exercitation ullamco laboris nisi ut aliquip ex ea commodo consequat. Duis aute irure dolor in reprehenderit in voluptate velit esse cillum dolore eu fugiat nulla pariatur. Excepteur sint occaecat cupidatat non proident, sunt in culpa qui officia deserunt mollit anim id est laborum.

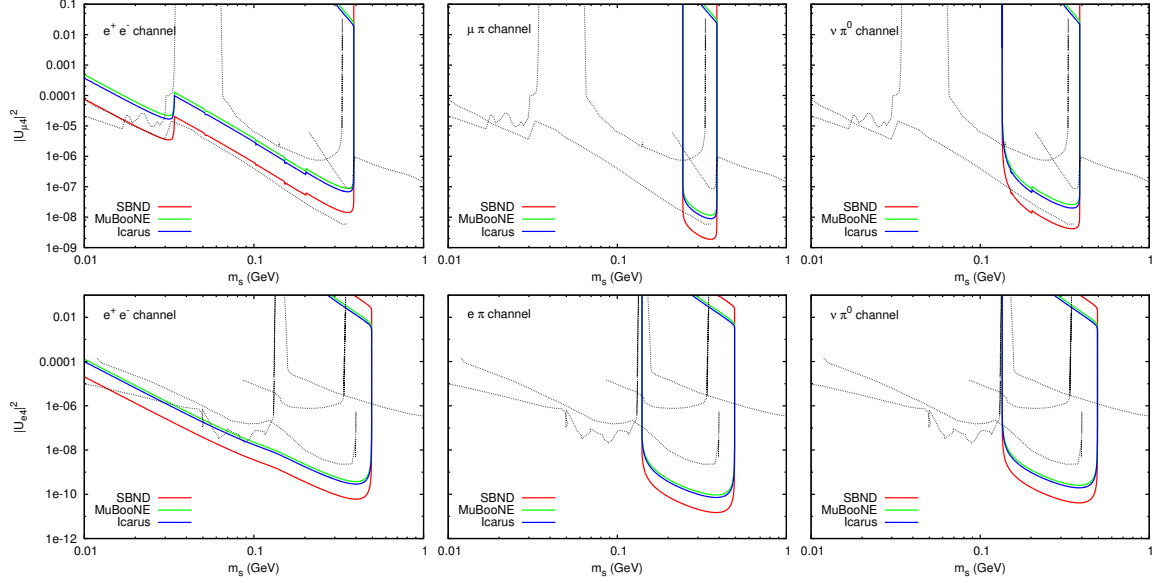


Figure 3. The sensitivity contours based on the total number of events, without cuts and without backgrounds. In all panels, the mixing matrix elements not shown on the y -axis are zero.

7 To do list

1. Actually compute a 95% CL exclusion region for a fair comparison with bounds. See comment directly below. (This isn't a total solution... but I spent a while reading about how to do this properly and I think it's pretty defensible. Perhaps more so than what we would do with log-likelihood ratios...).
2. The $S/\sqrt{B} = 1$ criterion is (if it's defensible at all) really a 1σ significance measure. I think we should at least switch it to $S/\sqrt{B} = 2$ which is $2\sigma \approx 95\%$ in the Gaussian limit. I have done this and updated the plotting scripts.
3. ~~Work out what has gone into the “cut-less” plots.~~ “Cut-less” plots have weight factors set to 1. Recompute for reasonable cuts? Vary the backgrounds according the cuts and Mark's estimates?
4. Turn on $U_{\tau 4}, U_{\mu 4}$ and $U_{e 4}$ simultaneously
5. ~~Edit how the code deals with cuts and efficiency files. “no-cuts” shouldn't need a dummy file of 1's. Maybe a flag “cuts-XXX” where XXX is either a file name, or “none” for which all is handled internally.~~ Now there is a “cuts” flag. “cuts=none” or “-cuts none” sets all weights to 1 internally. Or you can pass it a file name “cuts=eff.dat”, which works as expected. Default is no cuts, but I've updated the scripts to have the right flags.
6. ~~Write code for general Γ for different final state particles.~~ I've had a first pass at this. I didn't write new decay channels in the end, as I think we can just rescale things... depending on how we choose to scale the Γ with U and m (see below), we

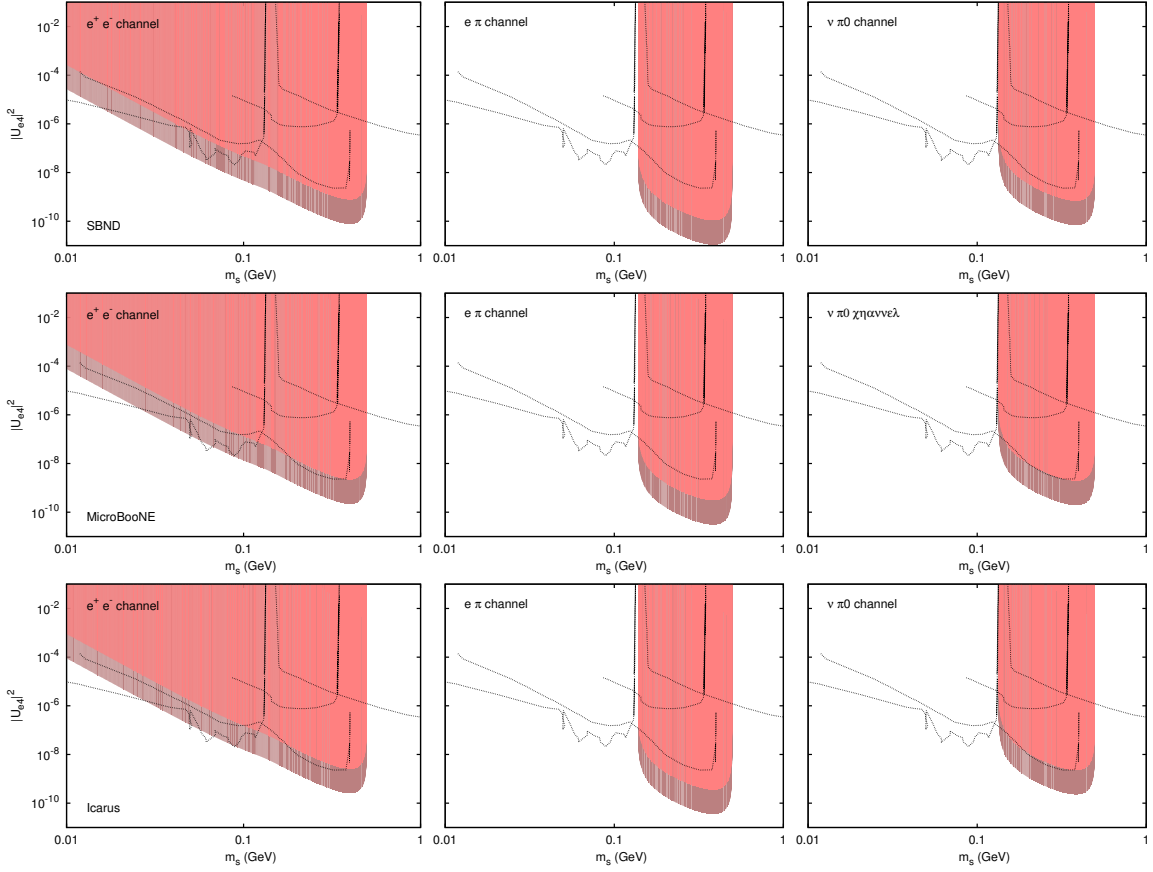


Figure 4. The sensitivity contours based on the total number of events, assuming only mixing with the electron neutrino ($|U_{\mu 4}|^2 = |U_{\tau 4}|^2 = 0$), without cuts but with varying degrees of background suppression. We overlay the 95% exclusion regions for U^2 and m_s from previous experimental work.

could change this later, but for now it seemed OK. Now there's a new command line argument which adds an extra Gamma to whichever channel you specify as well as the total decay rate *e.g.* `eventrate --mupi --extra-gamma 1e-18` adds a constant 1×10^{-18} to the $\mu\pi$ channel and total rate (not double counting). When we write a function like `loop_muon_enhanced_gamma()` we can set this extra gamma to depend on U or m as we need.

7. Write a section talking about the motivation for non-minimal extensions, specifically enhanced Γ . Discuss the breaking of the relationship between Γ , U^2 and m_s . Make a reasonable suggestion for possible scaling behaviours of Γ on U^2/m_s . Is it as boring as rewriting the minimal decay rate with G_F replaced by a new constant that isn't suppressed by the W -mass? Or can you get different scaling behaviours from new physics?
8. Based on the point above: decide how we can make plots for this. How do we compute the bounds? I guess, the bounds are *really* bounds on $U^2\Gamma$? What's the best way to display the three dimensional data etc. Make the data. Make the plots.

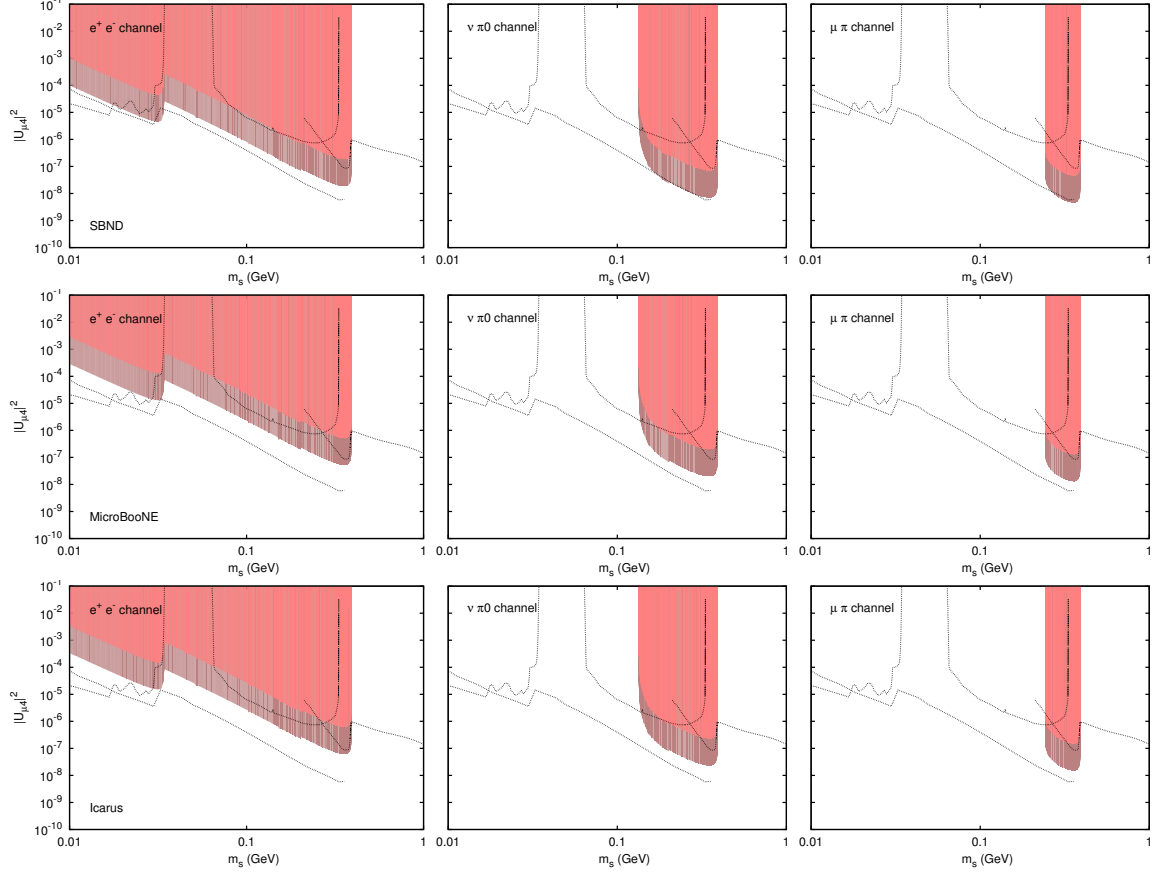


Figure 5. The sensitivity contours based on the total number of events, assuming only mixing with the muon neutrino ($|U_{e4}|^2 = |U_{\tau4}|^2 = 0$), without cuts but with varying degrees of background suppression. We overlay the 95% exclusion regions for U^2 and m_s from previous experimental work.

9. I have added the $(1 + \alpha)$ scaling functionality. I only ran one test... but it seems to work. I'll try to test more tomorrow.

References

- [1] M. Antonello *et al.* (LAr1-ND, ICARUS-WA104, MicroBooNE), (2015), [arXiv:1503.01520 \[physics.ins-det\]](#) .
- [2] R. Acciarri *et al.* (ArgoNeuT), *Phys. Rev. Lett.* **113**, 261801 (2014), [Erratum: *Phys. Rev. Lett.* 114, no.3, 039901 (2015)], [arXiv:1408.0598 \[hep-ex\]](#) .
- [3] H.-K. Tanaka, *Proceedings, 6th International Workshop on Neutrino-nucleus interactions in the few GeV region (NUINT 09)*, *AIP Conf. Proc.* **1189**, 255 (2009), [arXiv:0910.4754 \[hep-ex\]](#) .
- [4] C. T. Kullenberg *et al.* (NOMAD), *Phys. Lett.* **B682**, 177 (2009), [arXiv:0910.0062 \[hep-ex\]](#) .
- [5] G. J. Feldman and R. D. Cousins, *Phys. Rev.* **D57**, 3873 (1998), [arXiv:physics/9711021 \[physics.data-an\]](#) .